Anisotropy in the wet thermal oxidation of AlGaAs: influence of process parameters

Gael Lafleur, Guilhem Almuneau, Alexandre Arnoult, Henri Camon, Stéphane Calvez

Research Article | Vol. 8, No. 7 | 1 Jul 2018 | OPTICAL MATERIALS EXPRESS 1788
Optical Materials EXPRESS

Anisotropy in the wet thermal oxidation of AlGaAs: influence of process parameters

GAËL LAFLEUR, GUILHEM ALMUNEAU,* ALEXANDRE ARNOULT, HENRI CAMON, AND STÉPHANE CALVEZ

LAAS-CNRS, Université de Toulouse, CNRS, UPS, Toulouse, France
**almuneau@laas.fr*

Abstract: The crystallographic anisotropy of the lateral selective thermal oxidation of AlGaAs alloys is experimentally studied. The anisotropic behavior of this oxidation process, used primarily for building a lateral confinement in vertical surface emitting lasers (VCSEL), is quantified by varying different process parameters and the geometrical shapes of laterally oxidized mesa structures. This experimental study aims to have a better control of the oxide aperture shape used in oxide-confined photonics devices.

OCIS codes: (160.2100) Electro-optical materials; (160.6000) Semiconductor materials; (250.7260) Vertical cavity surface emitting lasers; (310.1860) Deposition and fabrication; (310.3840) Materials and process characterization; (310.2785) Guided wave applications; (230.4000) Microstructure fabrication.

References and links

1. J. M. Dallesasse and N. Holonyak, Jr., "Native-oxide stripe-geometry $Al_xGa_{1-x}As$-GaAs quantum well heterostructure lasers," Appl. Phys. Lett. **58**(4), 394–396 (1991).
2. P. D. Floyd, B. J. Thibeault, L. A. Coldren, and J. L. Mertz, "Scalable etched-pillar, AlAs-oxide defined vertical cavity lasers," Electron. Lett. **32**(2), 114–116 (1996).
3. K. D. Choquette, K. M. Geib, C. I. H. Ashby, R. D. Twesten, O. Blum, H. Q. Hou, D. M. Follstaedt, B. E. Hammons, D. Mathes, and R. Hull, "Advances in selective wet oxidation of AlGaAs alloys," IEEE J. Sel. Top. Quantum Electron. **3**(3), 916–926 (1997).
4. K. H. Ha, Y. H. Lee, H. K. Shin, K. H. Lee, and S. M. Whang, "Polarisation anisotropy in asymmetric oxide aperture VCSELs," Electron. Lett. **34**(14), 1401–1402 (1998).
5. P. Debernardi, J. M. Ostermann, M. Feneberg, C. Jalics, and R. Michalzik, "Reliable polarization control of VCSELs through monolithically integrated surface gratings: a comparative theoretical and experimental study," IEEE J. Sel. Top. Quantum Electron. **11**(1), 107–116 (2005).
6. C. L. Chua, R. L. Thornton, D. W. Treat, and R. M. Donaldson, "Anisotropic apertures for polarization-stable laterally oxidized vertical-cavity lasers," Appl. Phys. Lett. **73**(12), 1631–1633 (1998).
7. S. Weidenfeld, M. Eichfelder, M. Wiesner, W. M. Schulz, R. Rosbach, M. Jetter, and P. Michler, "Transverse-mode analysis of red-emitting highly polarized vertical-cavity surface-emitting lasers," IEEE J. Sel. Top. Quantum Electron. **17**(3), 724–729 (2011).
8. P. Nyakas, Z. Puskás, T. Kárpáti, T. Veszprémi, G. Zsombok, G. Varga, and N. Hashizume, "Optical simulation of vertical-cavity surface-emitting lasers with non-cylindrical oxide confinement," Opt. Commun. **250**(4–6), 389–397 (2005).
9. P. Nyakas, "Full-vectorial three-dimensional finite element optical simulation of vertical-cavity surface-emitting lasers," J. Lightwave Technol. **25**(9), 2427–2434 (2007).
10. P. Debernardi, G. P. Bava, C. Degen, I. Fischer, and W. Elsässer, "Influence of anisotropies on transverse modes in oxide-confined VCSELs," IEEE J. Quantum Electron. **38**(1), 73–84 (2002).
11. P. O. Vaccaro, K. Koizumi, K. Fujita, and T. Ohachi, "AlAs oxidation process in GaAs/AlGaAs/AlAs heterostructures grown by molecular beam epitaxy on GaAs (n11) A substrates," Microelectronics J. **30**(4–5), 387–391 (1999).
12. J. M. Dallesasse, P. Gavrilovic, N. Holonyak, Jr., R. W. Kaliski, D. W. Nam, E. J. Vesely, and R. D. Burnham, "Stability of AlAs in $Al_xGa_{1-x}As$-AlAs-GaAs quantum well heterostructures," Appl. Phys. Lett. **56**(24), 2436–2438 (1990).
13. W. Ranke, Y. R. Xing, and G. D. Shen, "Orientation dependence of oxygen absorption on a cylindrical GaAs crystal," J. Vac. Sci. Technol. **21**(2), 426–428 (1982).
14. F. Chouchane, G. Almuneau, N. Cherkashin, A. Arnoult, G. Lacoste, and C. Fontaine, "Local stress-induced effects on AlGaAs/AlOx oxidation front shape," Appl. Phys. Lett. **105**(4), 041909 (2014).
15. G. Almuneau, R. Bossuyt, P. Collière, L. Bouscayrol, M. Condé, I. Suarez, V. Bardinal, and C. Fontaine, "Real-time in situ monitoring of wet thermal oxidation for precise confinement in VCSELs," Semicond. Sci. Technol. **23**(10), 105021 (2008).

#325952 https://doi.org/10.1364/OME.8.001788
Journal © 2018 Received 12 Mar 2018; revised 25 May 2018; accepted 29 May 2018; published 7 Jun 2018

Optical Materials EXPRESS

16. A. C. Alonzo, X.-C. Cheng, and T. C. McGill, "Effect of cylindrical geometry on the wet thermal oxidation of AlAs," J. Appl. Phys. **84**(12), 6901–6905 (1998).
17. S. P. Nabanja, L. A. Kolodziejski, and G. S. Petrich, "Lateral oxidation of AlAs for circular and inverted mesa saturable Bragg reflectors," IEEE J. Quantum Electron. **49**(9), 731–738 (2013).
18. M. Osinski, T. Svimonishvili, G. A. Smolyakov, V. A. Smagley, P. Mackowiak, and W. Nakwaski, "Temperature and thickness dependence of steam oxidation of AlAs in cylindrical mesa structures," IEEE Photonics Technol. Lett. **13**(7), 687–689 (2001).
19. P. C. Ku and C. J. Chang-Hasnain, "Thermal oxidation of AlGaAs: modeling and process control," IEEE J. Quantum Electron. **39**(4), 577–585 (2003).
20. K. D. Choquette, K. M. Geib, C. I. Ashby, R. D. Twesten, O. Blum, H. Q. Hou, D. M. Follstaedt, B. E. Hammons, D. Mathes, and R. Hull, "Advances in selective wet oxidation of AlGaAs alloys," IEEE J. Sel. Top. Quantum Electron. **3**(3), 916–926 (1997).
21. S. Calvez, G. Lafleur, A. Larrue, P. F. Calmon, A. Arnoult, G. Almuneau, and O. Gauthier-Lafaye, "Vertically coupled microdisk resonators using AlGaAs/AlOx technology," IEEE Photonics Technol. Lett. **27**(9), 982–985 (2015).

1. Introduction

In many different AlGaAs-based photonic and optical devices, the selective oxidation of an Al-rich layer is a very efficient way to create a lateral electrical and optical confinement. The degree of confinement can thus be adjusted with the position in the stack and the lateral depth of the oxide within the structure. It is then of primary importance to control the lateral spreading of the oxidation reaction and this in all the crystallographic directions in order to define the waveguide properties in all three directions. If the vertical confinement can be designed through the choice of the index profile of the epitaxial multilayers, in the lateral directions (in the plane of the epilayers) only the kinetics of the selective oxidation controls the waveguide dimensions.

The crystallographic anisotropy in the reaction of wet thermal oxidation of Al(Ga)As is well known since the discovery of this process in the early 1990s' and, in particular, leads to an aperture shape which differs from the etched mesa from which the oxidation proceeds [1–3].

In oxide-confined Vertical-Cavity Surface-Emitting Lasers (VCSEL), an asymmetric shape of the confinement aperture has a strong impact on the properties of the output laser beam, positively as it may be a way to stabilize the polarization, or detrimentally as it modifies the transverse modes compared to a perfectly circular waveguide.

The polarization stabilization of the air-post (circular mesa, (100)-oriented) VCSEL emission has been a significant issue for many years because their quasi-symmetric geometry prevents the pinning of the beam polarization on a given direction. As a result, uncontrolled polarization switches can occur thereby reducing the device usefulness for many applications, in particular in optical communications. Several solutions have been proposed to solve this important issue, for example by introducing an asymmetric confinement by oxide or implantation [4], or by introducing a (polarizing) optical grating on the VCSEL surface [5]. Should the oxidation of the AlGaAs confinement layer be finely controlled in all the lateral directions, one could use an anisotropic shape of the oxide aperture to impose a polarization-stable emission. This has been practically achieved by oxidizing through etched holes appropriately located around the final aperture [6]. Some papers report on anisotropic elliptic aperture shapes that result in a preferential orientation of the laser mode profile in the direction of semi-major axis [7]. Some modelling works have considered the non-cylindrical oxide confinement, showing the incidences on the modal properties [8–10].

All these demonstrations, which reveal the strong importance of controlling the shapes of the area confined by the lateral oxidation, have been done by adapting the initial geometry of the etched pattern from which the lateral oxidation expands. This fine tuning of the mesa geometry leading to a given fixed shape of the oxide-confined waveguide can however be complex to implement.

In this paper, we complement the reported study on the anisotropy of the lateral oxidation of AlAs [11] by providing further experimental data on the oxidation of (<~100 nm)-thin

Optical Materials EXPRESS

AlGaAs layers to be in a position to make AlOx-based devices presenting controlled aperture shapes. In particular, the time evolution of the aperture shape is accurately extracted all along the oxidation process, providing useful insights on the kinetics of the oxidation reaction vis-à-vis its anisotropic behavior. We also explore the influence of the process parameters to establish the conditions which can lead to a more isotropic behavior.

2. Anisotropy in the AlOx process

The anisotropy of the oxidation process of AlGaAs compounds has been the subject of very few studies in spite of its high relevance for the photonic devices applications. It was first observed in [12] as a result of the exposure of thick AlAs/AlGaAs stacks to ambient air at room temperature for several years. The resulting oxidation/hydrolization of the Al-rich layers originating from point defects led to three-dimensional oxide boundaries that tend to be facetted on high-index plane crystallographic surfaces. A more specific study of the anisotropy was performed in [11]. The angular dependence of oxidation rates was measured for thin layers of AlAs grown on different substrate orientations, showing higher oxidation rates for the <100>, $[1\bar{1}1]$ and $[\bar{1}\bar{1}1]$ directions that correspond to the planes with metallic bonds. They also reported the influence of the oxidation temperature on the anisotropy, showing more isotropic behavior at low temperatures. These crystallographic effects, resulting in a higher oxidation rate along the <100> axes compared to <110> for AlAs, is consistent with the observations made in [13] where the different surface reactivity of oxygen atoms are showed to influence the oxidation of GaAs.

A well-known parameter impacting the anisotropy of the oxidation process is the composition of the alloy to-be-oxidized. For $Al_xGa_{1-x}As$ compounds, the process is found to become perfectly isotropic for Ga composition higher than 8% [3]. This composition effect can be explained by a modification of the neighbor atoms configuration in $Al_xGa_{1-x}As$ becoming significant for $x>0.92$.

Additionally, the oxidation rates can be affected by the mechanical stress resulting from the volumic shrinkage (of more than 10% for AlAs layers) that occurs during the oxidation. As an example, the shape of the oxidation front can be strongly modified by the strain-induced at the AlAs/AlOx interface as presented in [14]. This effect gives rise, for thick oxidized layers (>100 nm), to a strongly anisotropic oxidation front, which takes the form of a wedge whose interface is tilted of about 60° with respect to the wafer plane.

3. Experimental setup

The samples used in this study consist of a stack comprising a 70 nm AlAs or $Al_{0.98}Ga_{0.02}As$ capped with a 30 nm GaAs layer. This heterostructure is non-intentionally doped (NID) and grown by molecular beam epitaxy (Riber 412) under standard conditions (temperature, growth rate) on a NID (100) GaAs substrate.

The lateral selective oxidation of the (Al)GaAs layers is performed after an optical microlithography step to define the geometrical shape of the mesas. The spin-coated and lithographically-exposed SPR700 photoresist serves then as a mask for the subsequent etching step carried out by inductively-coupled plasma reactive-ion etching (ICP-RIE) in order to form the mesas thus releasing the sidewalls of the (Al)GaAs layer. This etching step is followed by a careful resist removal, and a surface cleaning with a diluted HCl solution (30s in HCl/H_2O 1:10) just before loading the sample in the oxidation chamber. This preparation is of prime importance to ensure reproducible surface conditions, and thus the repeatability of the start of the oxidation mechanisms.

The wet thermal oxidation is undertaken in a closed chamber under stabilized low pressure (in the 2-500 mbar range), where a controlled and constant mixed gas composed of water and forming gas (N_2/H_2 95/5%) is flown (AET Technologies). Both gas and liquid inlet flows are controlled by mass flow controllers, and the mixed moisture gas is generated by a CEM Bronkhorst system.

Optical Materials EXPRESS

The oxidation furnace is also equipped with a real-time in situ monitoring optical system [15], enabling the recording of the top-view of the mesa while oxidizing. In particular, in this study this monitoring system has been largely exploited to precisely follow the evolution of the oxidation front shape during the whole oxidation process until the whole surface of the mesa is oxidized. Based on the real-time acquired images of the oxidizing mesa, the full evolution of the profile of the oxidation edge is extracted by applying image numerical processing techniques and, in particular, an edge-detection based on the Sobel-Canny algorithm. This methodology enables to get the XY coordinates of the full oxidation edge contour with an accuracy limited by the lateral resolution of the magnifying optical system which has been estimated to be below 1 µm.

In this study, we spanned different process parameters, such as the time, temperature, chamber pressure, and moisture gas flow, as well as the initial geometry (circular mesa or void circular hole) to check their incidence on the anisotropy of the oxidation. Thanks to the real time monitoring system, the evolution of the oxidation front along all the lateral directions was traced with a high accuracy against time.

An example of these in situ acquired images is shown for three oxidation times on Fig. 1.

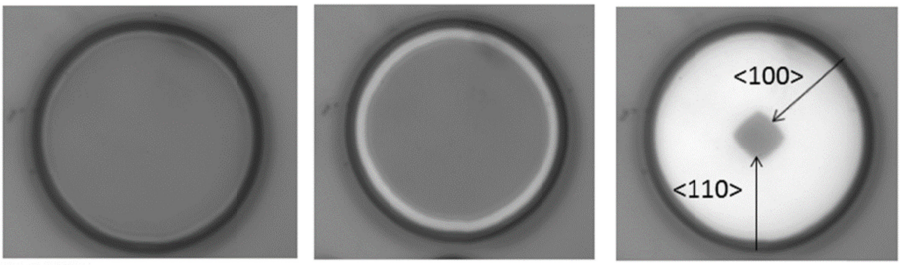

Fig. 1. In situ top images of laterally oxidized circular mesas during the oxidation process at three different process times. The mesa diameter is 60µm, and the oxidized zones appear in white.

As mentioned above, for a sample grown on (100)-oriented wafer, the oxidation anisotropy is primarily due to the different oxidation kinetics between the <100> and <110> directions. For an oxidation starting from a circular etched mesa, the anisotropy is quantified hereafter by the "square fraction", *s*, determining whether the oxide aperture shape (i.e. the boundary between the white and central pale-grey regions on Fig. 1) is akin to a circle (no anisotropy) or to a square (maximum anisotropy).

This parameter, defined with respect to the outer (circumscribed) circle and normalized between 0 and 1, is then obtained from the minimum and maximum aperture sizes (which occur respectively along the <110> and <100> directions) and expressed as:

$$s = \frac{|r_{<100>} - r_{<110>}|}{r_{<flat>} \cdot (1 - \frac{1}{\sqrt{2}})},$$

with $r_{<flat>} = r_{<110>}$ for an oxidation progressing inwards from an air-post mesa, and $r_{<flat>} = r_{<100>}$ for an oxidation progressing outwards from an etched hole.

4. Influences of experimental parameters

We study, thanks to the real-time monitoring of the oxidation front during the process, the evolution of the oxidation depth along the two main crystal orientations (<110> and <100>) between which the oxidation rate difference is maximum.

Optical Materials EXPRESS

Figure 2 depicts the time dependence measured for the inward oxidation of a 70-nm-thick AlAs layer carried out up to the full oxide closure from a 60-µm-diameter circular mesa. As previously reported and described by several papers [16,17], the oxidation evolves linearly, but tends to slightly accelerate when the aperture is about to close up. This effect, which deteriorates the process reproducibility when small apertures are targeted, is typical for mesa geometries for which the oxidizing front surface decreases against process time and can be reproduced by modelling [16–19]. This final stage acceleration varies with the process temperature and the oxidized layer thickness. In terms of anisotropy, Fig. 1 and 2.left show that the oxidation depths along the <100> and <110> directions differ and that their difference increases with oxidation time up to a time where the aperture size is about half that of the etched mesa. Beyond that point, the latter difference diminishes as a result of the reduction in oxide aperture size. Analyzing the oxide aperture shape in terms of the above-defined square fraction and taking into account the fact that the oxide contour can only be accurately determined for radii greater than ~5 µm (because of the monitoring system optical resolution), it becomes clear (see Fig. 2.right) that the oxidation reaction along the rapid crystal planes ({100}) prevails and forms an increasingly-square aperture whose edges are aligned to these preferential directions.

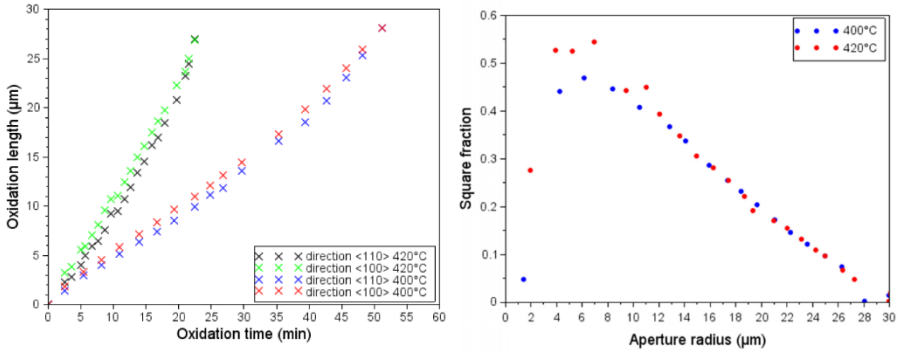

Fig. 2. left: Evolution during the process time of the oxidation depth along the <110> and <100> crystallographic directions for oxidations of a 70-nm-thick AlAs layer carried out from 30µm-radius mesa at a temperature of 400 and 420°C, a pressure of 500 mbar and a water flow of 5 g/h, and, right, associated anisotropy analysis in terms of square fraction.

This study is furthered by investigating the influence of the mesa geometry on the oxide aperture shape. In addition to straight ridges, two main cases have been considered: circular air-post mesas and etched holes whose radius is varied up to 100 µm.

The variation of the oxidation depths on these different geometries is reported on Fig. 3, as the function of the inversed radius, with negative values for etched holes, null value for straight stripe mesas, and positive values for air-post mesas. All these data points were measured on a set of mesas after a single 36-minute-long oxidation of an AlAs layer performed in standard conditions (400°C at 500 mbar).

Optical Materials EXPRESS

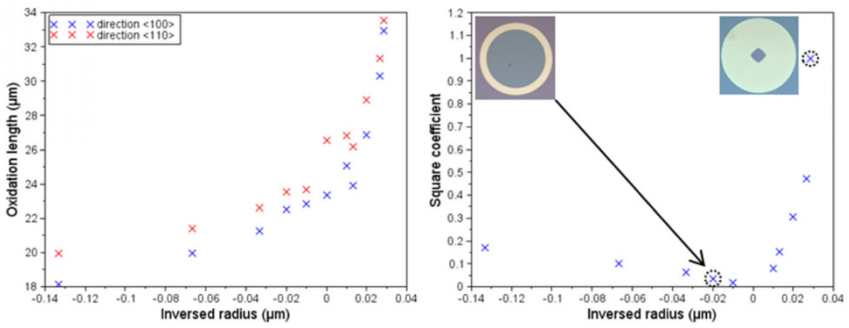

(a) (b)

Fig. 3. Oxidation depth evolution (a), and square fraction (*s*) against inverted radius of the mesa (b) (negative values of the radius is taken for etched holes)

Figure 3 shows that both the kinetics and the oxide front shape are strongly dependent on the initial mesa size. This variation could be assimilated to a linear dependence of the oxidation depth with the inverted initial mesa radius, with different slopes whether the mesa is air-post mesa or an etched hole. This difference in the kinetics between the both mesa configurations can be explained by a reaction-limited kinetic in the air-post configuration and by a diffusion-limited kinetic in the etched hole case.

As depicted on Fig. 3(b), the oxide aperture anisotropy also varies with the initial mesa radius. The evolution of the square fraction vs the inversed mesa radius is strongly asymmetric between air-post mesas and etched holes. For the air-post mesas, the aperture evolves rapidly to a square shape for small mesa diameters, while the oxidation from an etch holes has a much weaker variation towards square shape as the initial hole radius reduces.

Finally, we investigated the influence of the process parameters on the anisotropy. Once again, we capitalize upon the above-described experimental setup which enables a large number of process parameters such as the temperature, the moisture gas flow and the pressure of the oxidation chamber to be controllably varied. However, in this study, the to-be-oxidized layer was made of $Al_{0.98}Ga_{0.02}As$ (rather than an AlAs) since the former composition is the most commonly used in VCSEL fabrication and since the properties of the oxidation anisotropy seem to only be affected in magnitude.

The temperature, as shown in [11], has an important influence on the oxidation kinetics as it impacts simultaneously the chemical and the diffusion mechanisms of the oxidation process. We monitored the anisotropy of the aperture resulting from the oxidation of circular mesas as a function of temperature as shown on Fig. 4.

The results show the degree of anisotropy (i.e. square fraction *s*) of 6-µm-mean-diameter apertures starting from circular 35-µm-diameter mesas, when varying the temperature and the furnace chamber pressure. The temperature is not absolute as it is measured with a thermocouple placed in the heating susceptor holding the sample.

Figure 4 clearly shows a decreasing asymmetry in the aperture shape as the temperature increases. This result appears to contradict the results reported by Vaccaro [11], but might be explained by the fact that the composition of the oxidized layer is different ($Al_{0.98}Ga_{0.02}As$ here whilst it was AlAs in [11]) and effects related to the shape and size of the oxidized mesas (which are not explicitly mentioned in [11]).

We have also studied the impact on the anisotropy of other process-related parameters such as the chamber pressure (in the range of 4 to 800 mbar) and the moisture gas flow as these parameters have a large influence on the AlGaAs oxidation rate. If the chamber pressure and the process degree of anisotropy seemed to be uncorrelated, the moisture gas composition was seen to have a weak influence on the anisotropy (see inset of Fig. 4), with slightly more isotropic behavior observed for low water-vapor contents.

Optical Materials EXPRESS

In summary, these data suggest that the anisotropy of the oxidation of AlGaAs can be adjusted mainly through the process temperature, potentially reaching a fully isotropic behavior for temperatures above 500°C. Nevertheless, this high temperature range is not deemed to be compatible with the technological fabrication of devices like VCSELs as high-temperature treatments (under oxidizing atmosphere) are generally detrimental to device performance since they increase dopant diffusion, enhance the likelihood of (oxidation-inherent-)strain-induced damage, and promote the generation and propagation of dislocations. Additionally, from an oxidation perspective, as shown by Choquette et al. [20], the AlGaAs compositional selectivity of the oxidation process decreases at high temperatures, thereby induces an undesired over-oxidation of the low Al-content layers such as the low index layers of the top Bragg mirror. This effect, further compounded with an enhanced As surface desorption, can also lead to unwanted oxidation through point defects. Finally, as highlighted above, the higher the process temperature, the higher the oxidation rate and therefore tighter the process control need to be to maintain the manufacturing yield (i.e. to keep fabricating devices with a set aperture size and fixed tolerance bounds).

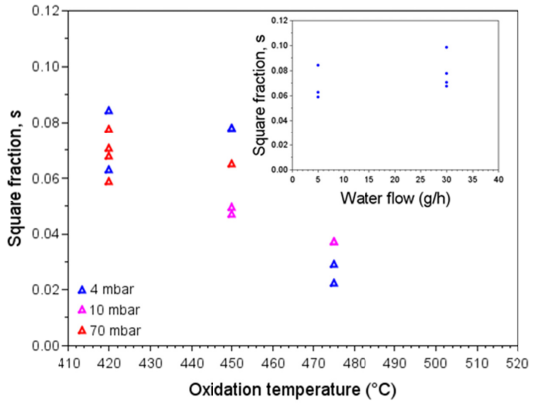

Fig. 4. Square fraction (anisotropy) of the oxide aperture (diameter around 6µm) obtained from a 35-µm-diameter $Al_{0.98}Ga_{0.02}As$ circular mesa versus process temperature, and (inset) versus water flow for a process temperature of 420°C .

5. Conclusion

In this work we have extracted the lateral spreading of the selective oxidation of high Al-content AlGaAs layers during the oxidation process. We then showed that the oxide aperture formed from a circular air-post mesa as standardly used in the VCSEL manufacturing process deforms to become a square as a result of the process anisotropy. We subsequently observed that the oxidation front geometry also depends on the shape of the mesa from which the oxidation proceeds. Finally, we led a study on the influence of the main parameters of the oxidation process on its anisotropic behavior by varying the temperature, moisture gas composition and chamber pressure. It was shown that high temperatures and low water-vapour content lead to more isotropic oxidations. This experimental study demonstrates the ability to tailor the geometry of the oxide confinement aperture in VCSELs, which, in turn, will affect the optical characteristics of the laser beam. In particular, a perfectly circular confinement oxide aperture will substantially improve the single mode performance, with improved mode selectivity and increased output power [10]. More generally, the presented knowledge of the anisotropic dependence of the AlGaAs oxidation on process parameters will also be beneficial to other types of oxide confined photonic devices [21] relying on more complex oxidation shapes as it enables a better control of the waveguide geometries.

Optical Materials EXPRESS

Funding

LAAS-CNRS.

Acknowledgements

This work was partly supported by the LAAS-CNRS micro and nanotechnologies platform, member of the French RENATECH network, and by the University Paul Sabatier for Gael Lafleur's PhD scholarship. The authors thank AET Technologies for technical assistance on the oxidation process.